

Article

Spatiotemporal Analysis of Extreme Hourly Precipitation Patterns in Hainan Island, South China

Wenjie Chen ¹, Chenghao Chen ², Longbing Li ², Litao Xing ², Guoru Huang ^{1,3,*} and Chuanhao Wu ¹

¹ School of Civil Engineering and Transportation, South China University of Technology, Guangzhou 510640, China; E-Mail: c.wenjie02@mail.scut.edu.cn

² Hydrology and Water Resources Survey Bureau of Hainan, Hainan 571126, China

³ State Key Laboratory of Subtropical Building Science, South China University of Technology, Guangzhou 510640, China

* Author to whom correspondence should be addressed; E-Mail: huanggr@scut.edu.cn; Tel.: +86-20-8711-4460.

Academic Editor: Athanasios Loukas

Received: 9 April 2015 / Accepted: 8 May 2015 / Published: 13 May 2015

Abstract: To analyze extreme precipitation patterns in Hainan Island, hourly precipitation datasets from 18 stations, for the period from 1967 to 2012, were investigated. Two precipitation concentration indices (PCI) and 11 extreme precipitation indices (EPI) were chosen. PCI1 indicated a moderate seasonality in yearly precipitation and PCI2 showed that at least 80% of the total precipitation fell in 20% of the rainiest hours. Furthermore, the spatial variations of PCI1 and PCI2 differed. Linear regression indicated increasing trends in 11 of the calculated EPI. Principal component analysis found that the first recalculated principal component represented the 11 EPI. The recalculated principal component revealed an increasing trend in precipitation extremes for the whole island (except the interior section). Trend stability analysis of several of EPI suggested that the southern parts of Hainan Island, and especially the city of Sanya, should receive more attention to establish the drainage facilities necessary to prevent waterlogging.

Keywords: extreme precipitation pattern; hourly datasets; extreme precipitation indices (EPI); principal component analysis (PCA); trend; stability

1. Introduction

Precipitation extremes are important hydrologic events, which receive a great deal of attention worldwide. The Intergovernmental Panel on Climate Change (IPCC) [1] indicated that the increasing frequency and intensity of extreme weather events is one of the major impacts of global warming. Keggenhoff [2] found that although the number of wet days in Georgia had decreased over the period of 1971 to 2010, the contribution of very heavy and extremely heavy precipitation to total precipitation had increased over the same period. Based on daily the precipitation records from 75 meteorological stations, Huang [3] indicated that both the frequency and intensity of the most extreme precipitation events showed an increasing trend in Hunan province, China. Results from the analyses of daily precipitation extremes in India by Sen Roy [4] were in general agreement with predictions from numerical models of increasing extreme precipitation events related to increasing concentrations of greenhouse gases in the atmosphere. Although much research has focused on extreme precipitation events in recent decades, short-duration rainstorms, which are one of the main factors leading to waterlogging, cannot be reliably described using daily precipitation datasets.

Characterized by a tropical monsoon climate, Hainan Island has an average annual precipitation of up to 1600 mm. Despite the very large amount of precipitation, there is extreme heterogeneity in monthly precipitation. Most of the rainfall occurs during the flood season. Furthermore, due to economic limitations, urban public facilities, especially drainage, tend to be underdeveloped in Hainan Island. The majority of Hainan residents are employed in the agricultural sector, with cereal crops covering the largest, most widely distributed area and being the most productive crops. Soil waterlogging causes this region to suffer from massive property and income losses. According to news reports, a rainstorm in 2010 affected 16 cities and caused economic losses of more than one billion yuan. Because of the urbanization and human activities on the island, precipitation extremes of short duration and high intensity, which can be learned from researching on hourly precipitation data rather than daily precipitation data, have an impact on urban hydrology and storm-water management [5]. Additionally, Beck *et al.* [5] also found that rainfall events exhibited different spatiotemporal characteristics in the early morning and in the afternoon, which cannot be described by daily precipitation data. Furthermore, precipitation is diverse temporally and spatially, so hourly data can reflect its variation more accuracy. However, almost no studies to date have focused on precipitation extremes in Hainan Island, based on hourly precipitation datasets. Therefore, we studied the spatial and temporal precipitation patterns in Hainan Island using hourly precipitation datasets, which could be used to inform prevention of waterlogging in the province.

2. Study Area and Datasets

2.1. Study Area

“Hainan”, which can literally be translated to “south of the sea”, is an island in the South China Sea (Figure 1). It is located between 18°10' N and 20°10' N, 108°37' E and 111°03' E, and is separated from Mainland China by a narrow strait. It covers an area of 35.4 thousand km². Characterized by a tropical monsoon and tropical oceanic climate, Hainan Island has an annual mean temperature of between 22 and 27 °C, and an annual mean precipitation of 1600 mm. The period from May to October is considered

to be the flood season in Hainan Island. The precipitation in the flood season can account for about 70% to 90% of annual precipitation. Hainan Island can be divided into three basins; the Nandu River basin, Changhua River basin and Wanquan River basin. These basins cover 47% of the total area of Hainan Island.



Figure 1. Locations of the precipitation stations in the study area.

2.2. Datasets

This study is based on the hourly datasets acquired from 18 precipitation stations over the period from 1967 to 2012. The locations of the 18 stations are shown in Figure 1, with additional details provided in Table 1. The tipping-bucket rain recorders and the siphon rainfall recorders, which could record the precipitation traces on the recording papers automatically, were the most commonly used in the measuring regions. Then, the precipitation traces were scanned into the computers and the hourly precipitation data could be extracted by extraction software. The dividing line for a rainy day was set at 8:00 P.M., and only the precipitation greater than 0.1 mm per hour could be recorded. Quality and homogeneity control was applied to the datasets using RCLimDex software (Climate Research Division, Environment Canada, Ottawa, ON, Canada) developed in “R” and presented by Wang and Feng [6]. The software can pick out the outliers and then we deal with these outliers using our judgment. The Illogical data, such as negative values, were treated as missing value. Less than 1% of the data was found to be missing for any station. The missing value was put to zero because it occupied less than 1% of the total data and would not have any effect on the calculation indices.

Table 1. Details of the precipitation stations in Hainan Island.

Station Name	Abbreviation	Longitude (°)	Latitude (°)	Elevation (m)
Baisha	BS	19.23	109.43	215.6
Baoting	BT	18.65	109.7	68.6
Changjiang	CJ	19.27	109.05	98.1
Chengmai	CM	19.73	110	31.4
Danzhou	DZ	19.52	109.58	169
Dingan	DA	19.7	110.33	24.2
Dongfang	DF	19.1	108.62	7.6
Ledong	LD	18.75	109.17	155
Lingao	LG	19.9	109.68	31
Lingshui	LS	18.5	110.03	13.9
Qionghai	QH	19.23	110.47	24
Qiongzong	QZ	19.03	109.83	250.9
Sanya	SY	18.22	109.58	419.4
Tunchang	TC	19.37	110.1	118.3
Wanning	WN	18.8	110.33	39.9
Wenchang	WC	19.62	110.75	21.7
Wuzhishan	WZS	18.77	109.52	328.5
Haikou	HK	20	110.25	63.5

To detect any clustering in the distribution of the selected stations, nearest neighbor analysis was undertaken. The nearest neighbor ratio was found to be 1.818, indicating that the distribution of stations displays a dispersed pattern at the 0.01 level of statistical significance.

3. Methods

3.1. Precipitation Concentration Indices (PCI)

In this study, two type of PCI are used to explore the changing patterns of precipitation concentration in Hainan Island. PCI1 is used to reveal monthly rainfall heterogeneity [7], while PCI2 is proposed to show hourly rainfall heterogeneity.

PCI1 is calculated as follows:

$$PCI1 = \frac{\sum_{i=1}^{12} P_i^2}{\left(\sum_{i=1}^{12} P_i\right)^2} \times 100 \quad (1)$$

where P_i is the monthly precipitation in month i . According to Equation (1), the minimum value of PCI1 is 8.3, which occurs when the same amount of precipitation falls in each month. Oliver [7] suggested that monthly rainfall heterogeneity could be divided into four categories according to the PCI1 values: uniform precipitation distribution ($PCI1 < 10$), moderate precipitation distribution ($PCI1: 10-15$), irregular precipitation distribution ($PCI1: 15-20$) and highly irregular precipitation distribution ($PCI1 > 20$).

PCI2 has been used to study daily rainfall heterogeneity [8], based on the fact that the precipitation frequency can generally be described by a negative exponential distribution (Equation (2)). In this study,

PCI2 is used to describe hourly rainfall heterogeneity, which is defined as the similarity between hourly and daily precipitation frequency distribution. We can find out that the relative between the accumulated percentages of precipitation Y and the accumulated percentages of hours X can be described by a negative exponential distribution (Figure 2).

$$Y = aX \exp(bX) \tag{2}$$

where a and b are constants.

According to Martin-Wide [8], PCI2 could be calculated as follows:

$$PCI2 = 1 - A' / 5000 \tag{3}$$

where A' is the definite integral of the exponential curve between 0 and 100.

$$A' = \left[\frac{a}{b} e^{bx} \left(x - \frac{1}{b} \right) \right]_0^{100} \tag{4}$$

$$\ln a = \frac{\sum X_i^2 \sum \ln Y_i + \sum X_i \sum (X_i \ln X_i) - \sum X_i^2 \sum \ln X_i - \sum X_i \sum (X_i \ln Y_i)}{N \sum X_i^2 - (\sum X_i)^2} \tag{5}$$

$$b = \frac{N \sum (X_i \ln Y_i) + \sum X_i \sum \ln X_i - N \sum (X_i \ln X_i) - \sum X_i \sum \ln Y_i}{N \sum X_i^2 - (\sum X_i)^2} \tag{6}$$

where N is the number of (X_i, Y_i) .

We can find out that the more heterogeneous in hourly precipitation, the smaller area A' will be. Thus, larger PCI2 value indicates more precipitation falls in a same period, showing more heterogeneous in hourly precipitation.

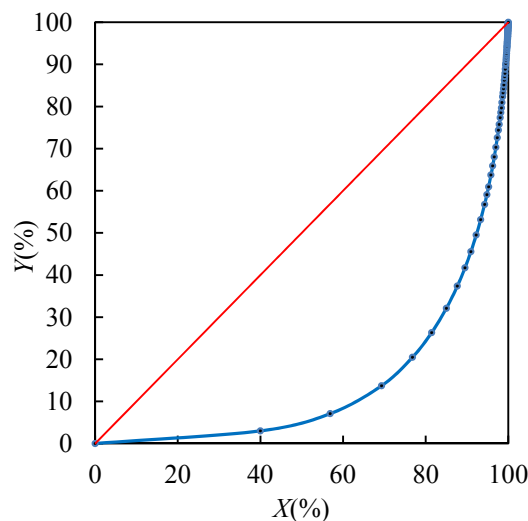


Figure 2. Accumulated percentages of precipitation Y —accumulated percentages of hours X curve (Blue curve represents the heterogeneous precipitation. Red curve represents the perfectly homogeneous precipitation.).

3.2. Extreme Precipitation Indices

A review of the methods used to test trends in extreme precipitation patterns regionally suggests that certain threshold values can be used to identify extreme values. For example, Haylock *et al.* [9] utilized two indices of extreme rainfall, which were calculated from daily precipitation data during the period from 1958 to 2000 in Europe. In another study by Sen Roy [10], nine extreme precipitation variables based on hourly datasets were utilized. Given the variety of indices that have been used to determine trends in extreme hourly precipitation values in combination with local conditions, the following indices have been used in this study (Table 2).

Table 2. Extreme precipitation indices (EPI) used in the current study. All precipitation events greater than 0.1 mm occurring throughout the entire study period were sorted in ascending order for each station separately to determine the percentile threshold values.

Index	Definition	Unit
FQ 90	Frequency of precipitation greater than the 90th percentile threshold value during the flood season	h
FQ 95	Frequency of precipitation greater than the 95th percentile threshold value during the flood season	h
FQ 97.5	Frequency of precipitation greater than the 97.5th percentile threshold value during the flood season	h
TP 90	Total amounts of precipitation greater than the 90th percentile threshold value during the flood season	mm
TP 95	Total amounts of precipitation greater than the 95th percentile threshold value during the flood season	mm
TP 97.5	Total amounts of precipitation greater than the 97.5th percentile threshold value during the flood season	mm
Max 1 h	Largest hourly precipitation during the flood season	mm
Max 3 h	Largest continuous 3-h precipitation during the flood season	mm
Max 6 h	Largest continuous 5-h precipitation during the flood season	mm
FQ 20 mm	Frequency of hourly precipitation during the flood season greater than 20 mm	h
FQ 30 mm	Frequency of hourly precipitation during the flood season greater than 30mm	h

3.3. Principal Component Analysis (PCA)

For each station, a matrix of 46 rows corresponding to each year from 1967 to 2012, and 12 columns containing the year and each of the 11 EPI described above was compiled. Linear regression analysis was then carried out for each station. A matrix of 18 rows, one for each station, and 12 columns, containing the year and the standardized regression coefficients was then compiled for each index. The standardized regression coefficients, calculated as the unstandardized regression coefficients multiplied by (S_x/S_y) , where S_x is the standard deviation of the independent variable and S_y is the standard deviation of the dependent variable, represent the strength of the trend.

Table 3 presents the correlation coefficients for the 11 EPI. As shown in Table 3, all of the coefficients are greater than 0.5, indicating that they are suitable for inclusion in PCA. PCA was applied to the new 18-row by 12-column matrix. The first component calculated through PCA explained 82% of the

variation for the 11 EPI. The loading matrix of standardized regression coefficients is shown for the first component in Table 4. All variables have loadings higher than 0.7, suggesting that the first component reflects both the frequency and the intensity of extreme precipitation. Finally, we recalculated [4] the component scores by setting their standard deviation to 0.14 (the mean standard deviation of the 11 EPI) and their mean to 0.23 (the average mean of the 11 EPI).

Table 3. Correlation coefficients of the extreme precipitation indices (EPI).

Correlation Coefficient	FQ 90	FQ 95	FQ 97.5	TP 90	TP 95	TP 97.5	Max 1 h	Max 3 h	Max 6 h	FQ 20 mm	FQ 30 mm
FQ 90	1.000	--	--	--	--	--	--	--	--	--	--
FQ 95	0.942	1.000	--	--	--	--	--	--	--	--	--
FQ 97.5	0.857	0.858	1.000	--	--	--	--	--	--	--	--
TP 90	0.946	0.913	0.930	1.000	--	--	--	--	--	--	--
TP 95	0.908	0.923	0.934	0.988	1.000	--	--	--	--	--	--
TP 97.5	0.810	0.788	0.949	0.948	0.956	1.000	--	--	--	--	--
Max 1 h	0.732	0.668	0.702	0.829	0.806	0.805	1.000	--	--	--	--
Max 3 h	0.728	0.629	0.806	0.822	0.790	0.852	0.817	1.000	--	--	--
Max 6 h	0.698	0.580	0.750	0.772	0.732	0.791	0.650	0.923	1.000	--	--
FQ 20 mm	0.816	0.806	0.922	0.918	0.927	0.944	0.697	0.826	0.777	1.000	--
FQ 30 mm	0.580	0.558	0.608	0.762	0.783	0.808	0.748	0.698	0.661	0.788	1.000

Table 4. Loadings of the standardized regression coefficients.

EPI	FQ 90	FQ 95	FQ 97.5	TP 90	TP 95	TP 97.5	Max 1 h	Max 3 h	Max 6 h	FQ 20 mm	FQ 30 mm
Loading	0.907	0.873	0.938	0.987	0.979	0.969	0.845	0.889	0.833	0.946	0.798

3.4. Stability Test

The Mann-Kendall (M-K) trend test [11,12], recommended by the World Meteorological Organization (WMO), is an effective tool to assess the significance of monotonic trends in hydrometeorological time series. This method has the advantages of not requiring a given data distribution and not being affected by outlying data, and has been used extensively to test trends in hydrometeorological data, including temperature, rainfall and runoff time series [13–16]. In this study, the M-K method was used to test the trend stability of extreme precipitation time series.

In general, the trend of a time series is detected for a specific time period, and test results are strongly influenced by the selection of the latter. For the same variable, it is likely that different trends will result from the analysis of different time periods, which reflects the instability of the trend. It is, therefore, difficult to determine the real trend of a time series. To access the stability characteristics of trends evaluated in this study, we determined the stability of extreme temperature and precipitation trends using the statistical significance of the trends tested by the M-K method, following the approach of Lupikasza [17] and Hidalgo-Muñoz *et al.* [18]. In this method, trend stability was defined as follows:

$$S = \frac{N_{0.1}}{K} \tag{7}$$

where K is the number of 30-year moving periods for one station (17 movable 30-year periods during the 1967–2012 period) and No.1 is the number of 30-year moving periods for each trend direction that passes the M-K test at the 90% confidence level. Trends are categorized as unstable ($S < 0.25$), stable ($0.25 \leq S < 0.6$), or highly stable ($S \geq 0.6$).

4. Results and Discussion

4.1. Spatial Pattern of PCI for 1967–2012

As is well known, Hainan Island is characterized by a tropical monsoon climate, which has distinct wet and dry seasons. To understand precipitation patterns in Hainan Island, we calculated of two PCI, PCI1 and PCI2.

4.1.1. PCI1

Figure 3 shows the spatial distributions of both calculated PCI. Throughout the island, PCI1 values range from 11.8 to 14.7. According to Oliver [7], such PCI1 values indicate a moderate precipitation distribution in Hainan Island. The maximum PCI1 value was found for the Western Changjiang County, while the minimum value was recorded for the Northeastern Wenchang County. Moreover, the seasonal precipitation concentration presents a decreasing trend from west to east.

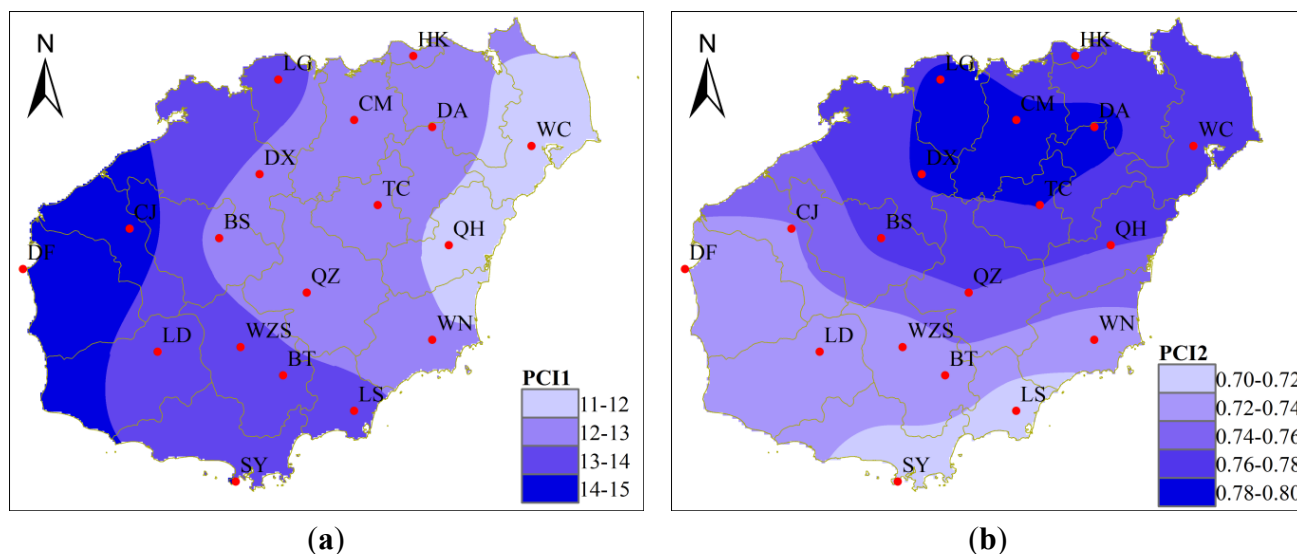


Figure 3. The spatial distribution of (a) PCI1 and (b) PCI2 from 1967 to 2012.

4.1.2. PCI2

PCI2 is applied to explore the contribution of precipitation extremes of certain lengths of time to total precipitation. Zhang *et al.* [19] found the lowest PCI2 values in the southwestern and northeastern regions of the Pearl River basin and the highest values in the northwestern and southern regions over the period 1960–2005. However, PCI2 values in Hainan Island are between 0.70 and 0.79, and display an obvious increasing trend from south to north, which is different from that of PCI1. The north-central regions of Hainan Island are characterized by the maximum PCI2 values, which are all above 0.78. On the contrary, the southern regions are characterized by the lowest values, below 0.72. Furthermore,

PCI2 was proposed to reflect the contribution of hours with the highest rainfall to the total amount of precipitation. In this study area, the PCI2 value of 0.70 corresponds with 80% of total precipitation falling in the 20% rainiest hours.

Due to the temporal heterogeneity of precipitation, the rest of this article focuses on analyzing precipitation extremes in the flood season (May to October).

4.2. Extreme Precipitation Indices (EPI) Trends

This section is devoted to the trends and significances thereof of the EPI calculated for the study region. The magnitude of the trends was calculated using linear regression analysis, which reveals the trend direction and the magnitude of variation of precipitation extremes. The M-K test was used to evaluate the trend significance. In recent years, several studies have undertaken similar work. For example, Chi *et al.* [20] used the generalized least squares method to analyze the linear regression trends, and found an increase in the frequency of extreme precipitation and a reduction in the frequency of light rain days in eastern forest regions of China in recent 50 years. Gocic *et al.* [21] analyzed precipitation and standardized precipitation index trends using linear regression in Serbia.

4.2.1. Statistical Trends

Regional precipitation indices, which are plotted in Figure 4, exhibit increasing trends. This result aligns with the statement of IPCC [1], that global warming has led to an increasing frequency and intensity of extreme precipitation events. The frequency indices investigated here, including FQ 90, FQ 95, FQ 97.5, FQ 20 mm and FQ 30 mm (Figure 4), show increasing trends for the whole island. The increasing rates of the five indices listed above are 2.5 h/decade, 1.4 h/decade, 1.1 h/decade, 1.2 h/decade and 0.6 h/decade, respectively. For TP 90, TP 95 and TP 97.5, rapidly increasing rates of 5.2 mm/year, 4.3 mm/year and 3.7 mm/year, respectively, can be observed. The Max 1 h, Max 3 h and Max 6 h display increasing rates of 1.9 mm/decade, 3.1 mm/decade and 4.6 mm/decade, respectively. In other words, both the frequency and the intensity of extreme precipitation events exhibit increasing trends. Furthermore, it also can be seen that almost all of the indices present the rapidly increase after 1987. It is more likely an oscillation in the long term variations instead of a tipping point. Shinjiro [22] found that the conclusion recent heavy precipitation in the 1990s was unprecedentedly intense and frequent in Tokyo was misunderstanding. He digitalized hourly precipitation since 1890 recorded at the Tokyo observatory and concluded that the local frequency minimum in the longer time series is just located in the 1970s. The 1990s was not the tipping point instead of a long-term cycle. In addition to Tokyo, Zhu [23] researched on summer monsoon rainfall in China and found an 80-year scale variability. Minobe [24] found a 50–70 year climatic oscillation over the North Pacific and North America. We can observe a 20-year oscillation in the precipitation extremes through the five-year moving average lines.

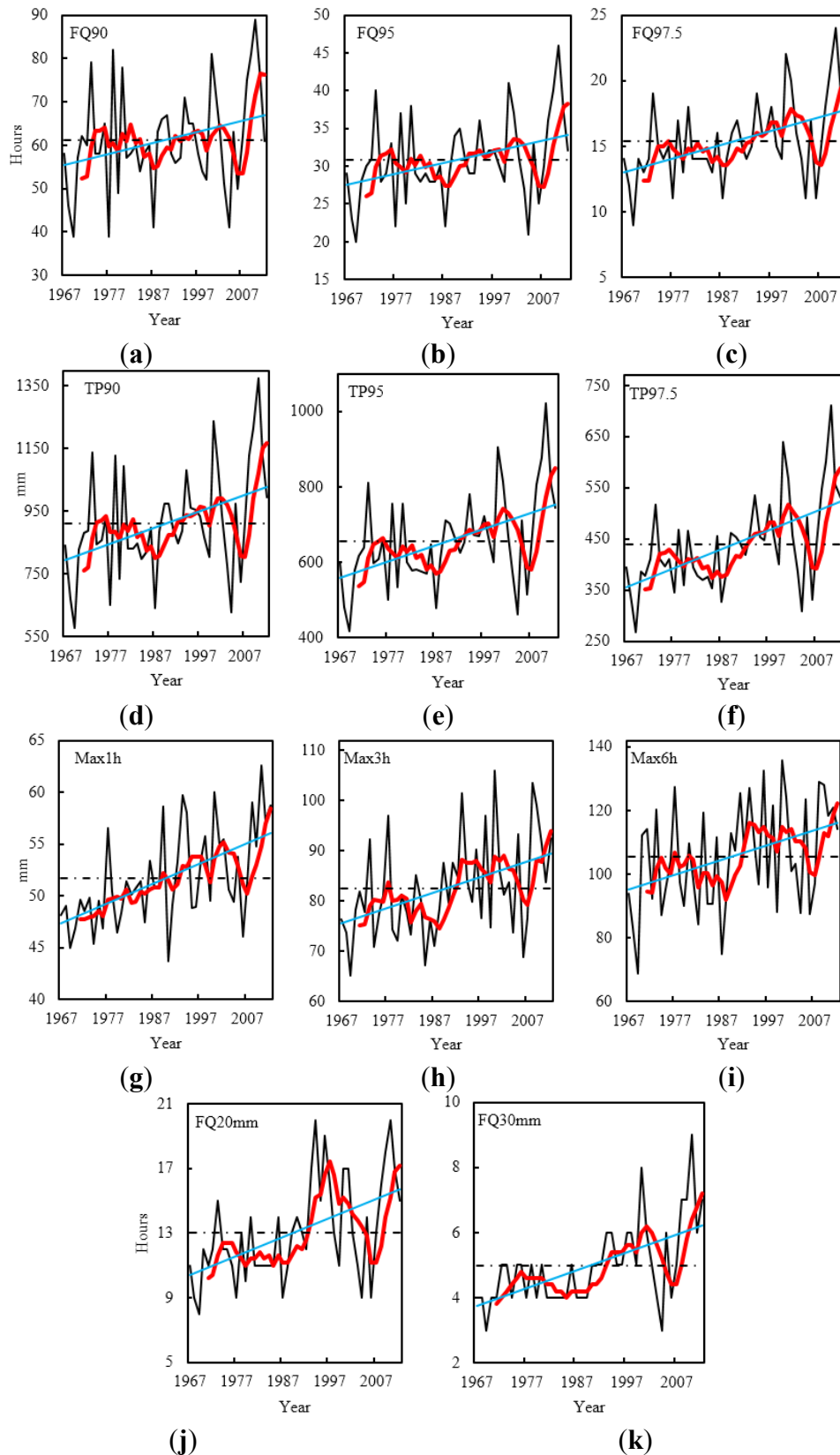


Figure 4. Regional time series of EPI for the flood season. (Black curves represent the arithmetic average of all station. Red curves represent the 5-year moving average. Blue lines are the trend lines of the indices. Black dotted lines show the 1967–2012 average.) (a) FQ 90; (b) FQ 95; (c) FQ 97.5; (d) TP 90; (e) TP 95; (f) TP 97.5; (g) Max 1 h; (h) Max 3 h; (i) Max 6 h; (j) FQ 20 mm; (k) FQ 30 mm.

4.2.2. Trend Significance

Table 5 shows the results of the trends significant tests for the regional EPI. All trends are significant at the 0.1 level, indicating that all the EPI display significant increasing trend. Only the FQ 90 is significant at the 0.1 level, whereas FQ 95 and Max 6 h are significant at the 0.05 level, and all others are significant at 0.01 level.

Table 5. Results of the trend significance tests for the regional EPI for the period 1967–2012.

EPI	FQ 90	FQ 95	FQ 97.5	TP 90	TP 95	TP 97.5	Max 1 h	Max 3 h	Max 6 h	FQ 20 mm
Z value	1.79 *	2.49 **	3.31 ***	2.84 ***	3.26 ***	3.60 ***	4.07 ***	2.78 ***	2.36 **	3.42 ***
Statistical trends	Sut	Sut	Sut	Sut	Sut	Sut	Sut	Sut	Sut	Sut

Notes: Z value is calculated by the M-K test. Sut, significant upward trends. * Significant at the 0.1 level; ** Significant at the 0.05 level; *** Significant at the 0.01 level.

4.3. Spatial Patterns of the Trends

The first component reflects most of the variation of EPI. Sen Roy [4] calculated the first component using seven EPI as input to describe the trends of precipitation extremes in India. To determine the spatial patterns of trends in the Hainan Island, the recalculated first component is plotted (Figure 5). The recalculated first component, ranging from -0.101 to 0.458 , shows that the regression coefficients are generally positive in the northern and southern regions of Hainan Island, while the interior regions experience negative trends. Negative trends are also observed in LG and DF stations, which are located in the northern and eastern regions, respectively. CM, WC and SY stations exhibit the most positive trends. On the contrary, QZ station displays the most negative trend.

The maximum amount of precipitation occurring within a specified time period is one of the most common methods used to define extreme precipitation events [25]. Accordingly, to display the patterns of extreme precipitation in Hainan Island, we have also mapped three other EPIs, FQ 20 mm, TP 90 and Max 3 h (Figure 5). Spatial patterns of these three indices are similar, and show positive trends in the northern and southern regions, and negative trends in the interior regions. However, small differences exist for some stations. For example, LG station shows positive trends for FQ 20 mm and Max 3 h, and a negative trend for TP 90.

Moreover, the decreasing trends are observed to concentrate predominantly in interior section, where the elevation is higher than the surrounding coastal areas. Many people researched on the relationships between elevation and trends of EPI. Zhang *et al.* [26] researched precipitation extremes over the Hengduan mountains region and found that trends of some precipitation indices displayed statistically negative correlation with elevation while trends of some other indices showed positive correlation with elevation. However, in the paper of Chen *et al.* [27], they found that each EPI showed a different fluctuation in trend with elevation and they concluded that no significant correlations between trends of EPI and elevation. The elevation of the interior stations, such as BS, QZ and WZS, is usually higher than 200 m while the elevation of the coastal areas (except SY station) is lower than 200 m. It may therefore be concluded that high elevations have decreasing trends in precipitation extremes. However, this is not the case for all stations. For example, SY station is a coastal station with an elevation greater than 200 m, but shows an increasing trend. Furthermore, trends of EPI are associated with not only the elevation but also

trends of annual precipitation. We then find that annual precipitation in QZ station exhibits decreasing trends from 1967 to 2012 while others exhibit increasing trends. The decreasing trend in annual precipitation is the main cause leading to the decreasing trend in precipitation extremes in QZ. We may venture to conclude that there is no significant correlation between elevation and trends of EPI.

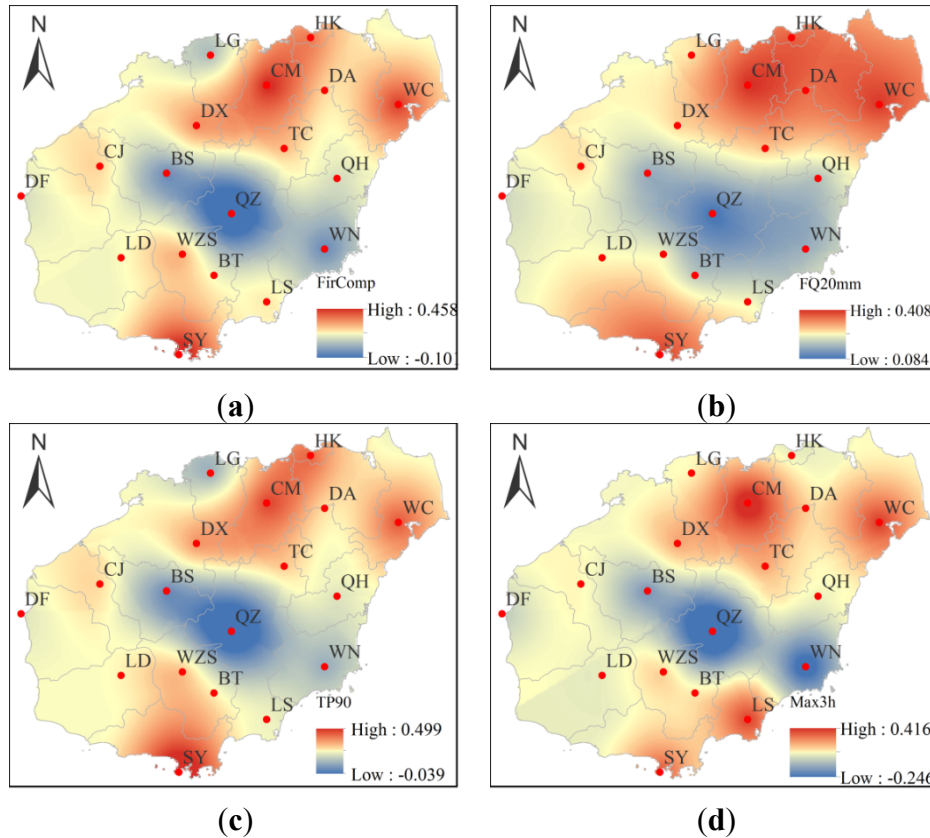


Figure 5. Flood season spatial patterns of trends in (a) the PCA first component; (b) FQ 20 mm; (c) TP 90 and (d) Max 3 h.

4.4. Trend Stability

To better illustrate the spatial patterns of extreme precipitation, the trend stability was also analyzed. Distinct from their trend distributions, the stabilities of FQ 20 mm, Max 3 h and TP 90 are dissimilar in Hainan Island (Figure 6). However, instabilities are present in most regions. The stability coefficients of FQ 20 mm in the northeastern and southwestern regions are between 0.25 and 0.6. As described by Wu [28], stability coefficients ranging from 0.25 to 0.6 indicate a stable trend. Most regions of Hainan Island show an unstable trend for Max 3 h. In the southern region, BT, LS and SY stations, show stable trends. For TP 90, stations associated with stable trends are located in the northern and southern regions of the study area. SY station exhibits strong stability for TP 90. Furthermore, combined with the increasing trend revealed in the previous section, the SY station shows a strongly stable increasing trend for 1967–2012. The stability in FQ 20 mm exhibits a similar phenomenon to TP 90, but the area for which stable trends are calculated is larger. Overall, most regions of Hainan display unstable EPI trends, while some parts of the southern and northern regions exhibit stable or strongly stable trends.

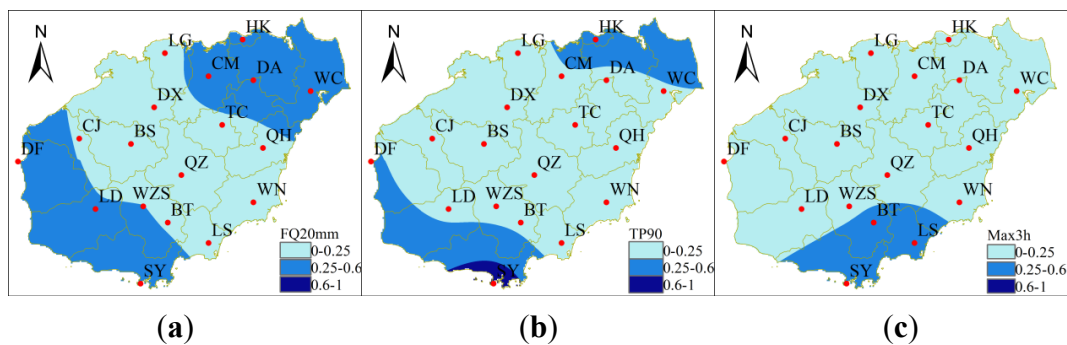


Figure 6. Trend stability for (a) FQ 20 mm; (b) TP 90 and (c) Max 3 h over the study period.

5. Conclusions

The precipitation heterogeneity and the spatial and temporal distribution of trend directions in precipitation extremes in Hainan Island during the period 1967–2012 were analyzed using two PCI and 11 EPI. In line with IPCC findings [1], the frequency and intensity of extreme precipitation events was found to exhibit increasing trends corresponding with observed global warming. According to Wu *et al.* [29], extreme events contribute significantly to variations in the extreme precipitation amount, as well as in the total annual precipitation. During the period from 1962 to 2005, both the number of days and the total precipitation associated with extreme events slightly increased in Hainan Island. Additionally, we also found a possible conclusion that a 20-year oscillation existed in precipitation extremes. Further investigation in the precipitation extremes oscillation is indispensable.

PCI1 in Hainan Island ranges from 11.8 to 14.7, indicating that yearly precipitation displays a moderate seasonality. PCI1 presents a decreasing trend from Western to Eastern Hainan. Precipitation in the western region of Hainan is known to be characterized by severe seasonality, while the seasonality of the southern region is known to be less severe. However, different trends appear in PCI2, which is calculated to reveal the concentration of hourly precipitation. Ranging from 0.70 to 0.79, PCI2 generally showed an increasing trend from south to north. In other words, more precipitation falls in a shorter period in the north, suggesting that more short-duration storms occur in this region. Wu *et al.* [29] also found that the heaviest 1% of daily precipitation contributes 23% of the annual precipitation in Hainan Island. In our study, at least 80% of the total precipitation is found to fall in the 20% rainiest hours. Overall, through the analysis of PCI1 and PCI2, it can be concluded that precipitation in the western region is more seasonal than in the eastern region, and that the northern hourly precipitation is more concentrated than that of the southern region.

Overall, for the entire island, it was observed that precipitation extremes show significant increasing trends. However, similar to the spatial patterns of precipitation extremes in Hainan Island, the southern and northern regions exhibit increasing trends, while the interior exhibits a decreasing trend. In other words, in the southern and northern Hainan Island, the frequency, amount, and intensity of rainstorms showed increasing trends for the period 1967–2012, which is the opposite of the interior region. Additionally, there is no significant correlation between elevation and trends of EPI.

Furthermore, an increasing trend of precipitation extremes can be predicted through the trend uncovered for the past decades and related trend stability. The northern and southern regions should receive more attention to prevent potential damage inflicted by the precipitation extremes according to the combination of statistical trends and stabilities. A strongly stable increasing trend in TP 90 for SY

station indicates that the amount of precipitation in rainstorms can be expected to increase steadily, which may cause waterlogging in Sanya county.

Acknowledgments

This study has been financially supported by the Ministry of Water Resources Special Funds for Scientific Research Projects of Public Welfare Industry (201301093 and 201401048).

Author Contributions

Authors collaborated together for the completion of this work. Wenjie Chen designed this study, processed data and wrote the manuscript. Chenghao Chen, Longbing Li and Litao Xing provided the precipitation data, processed data and contributed to the EPI calculation. Guoru Huang designed the study, reviewed and revised the manuscript. Chuanhao Wu contributed to the EPI calculation, reviewed and revised the manuscript.

Conflicts of Interest

The authors declare no conflict of interest.

References

1. Working Group I Contribution to the Fifth Assessment Report of the Intergovernmental Panel on Climate Change. Available online: http://www.ipcc.ch/pdf/assessment-report/ar5/wg1/WG1AR5_Frontmatter_FINAL.pdf (accessed on 12 May 2015).
2. Keggenhoff, I.; Elizbarashvili, M.; Amiri-Farahani, A.; King, L. Trends in daily temperature and precipitation extremes over Georgia, 1971–2010. *Weather Clim. Extrem.* **2014**, *4*, 75–85.
3. Huang, J.; Sun, S.L.; Xue, Y.; Zhang, J.C. Spatial and temporal variability of precipitation indices during 1961–2010 in Hunan province, Central South China. *Theor. Appl. Climatol.* **2014**, *118*, 581–595.
4. Sen Roy, S.; Balling, R.C. Trends in extreme daily precipitation indices in India. *Int. J. Climatol.* **2004**, *24*, 457–466.
5. Beck, F.; Bárdossy, A.; Seidel, J.; Müller, T.; Fernandez Sanchis, E.; Hauser, A. Statistical analysis of sub-daily precipitation extremes in Singapore. *J. Hydrol. Reg. Stud.* **2015**, *3*, 337–358.
6. RClimDex. Available online: <http://etccdi.pacificclimate.org/software.shtml> (accessed on 17 November 2013).
7. Oliver, J.E. Monthly precipitation distribution: A comparative index. *Prof. Geogr.* **1980**, *32*, 300–309.
8. Martin-Vide, J. Spatial distribution of a daily precipitation concentration index in peninsular Spain. *Int. J. Climatol.* **2004**, *24*, 959–971.
9. Haylock, M.R.; Goodess, C.M. Interannual variability of European extreme winter rainfall and links with mean large-scale circulation. *Int. J. Climatol.* **2004**, *24*, 759–776.
10. Sen Roy, S.; Rouault, M. Spatial patterns of seasonal scale trends in extreme hourly precipitation in South Africa. *Appl. Geogr.* **2013**, *39*, 151–157.
11. Mann, H.B. Non-parametric tests against trend. *Econometrica* **1945**, *13*, 245–259.
12. Kendall, M.G. *Rank Correlation Methods*, 4th ed.; Charles Griffin: London, UK, 1975.

13. Wan, L.; Zhang, X.P.; Ma, Q.; Zhang, J.J.; Ma, T.Y.; Sun, Y.P. Spatiotemporal characteristics of precipitation and extreme events on the loess plateau of china between 1957 and 2009. *Hydrol. Process.* **2014**, *28*, 4971–4983.
14. Bocchiola, D. Long term (1921–2011) hydrological regime of alpine catchments in northern Italy. *Adv. Water Resour.* **2014**, *70*, 51–64.
15. Taxak, A.K.; Murumkar, A.R.; Arya, D.S. Long term spatial and temporal rainfall trends and homogeneity analysis in wainganga basin, Central India. *Weather Clim. Extrem.* **2014**, *4*, 50–61.
16. Anghileri, D.; Pianosi, F.; Soncini-Sessa, R. Trend detection in seasonal data: From hydrology to water resources. *J. Hydrol.* **2014**, *511*, 171–179.
17. Lupikasza, E. Spatial and temporal variability of extreme precipitation in Poland in the period 1951–2006. *Int. J. Climatol.* **2010**, *30*, 991–1007.
18. Hidalgo-Munoz, J.M.; Argueso, D.; Gamiz-Fortis, S.R.; Esteban-Parra, M.J.; Castro-Diez, Y. Trends of extreme precipitation and associated synoptic patterns over the Southern Iberian Peninsula. *J. Hydrol.* **2011**, *409*, 497–511.
19. Zhang, Q.; Xu, C.Y.; Gemmer, M.; Chen, Y.D.; Liu, C.L. Changing properties of precipitation concentration in the pearl river basin, China. *Stoch. Environ. Res. Risk A* **2009**, *23*, 377–385.
20. Chi, Y.; Zhang, C.; Liang, C.; Wu, H. The precipitation change in eastern forest regions of China in recent 50 years. *Acta Ecol. Sin.* **2013**, *33*, 217–226.
21. Gocic, M.; Trajkovic, S. Analysis of precipitation and drought data in Serbia over the period 1980–2010. *J. Hydrol.* **2013**, *494*, 32–42.
22. Shinjiro Kanae, T.O.; Akira, K. Changes in hourly heavy precipitation at Tokyo from 1890 to 1999. *J. Meteorol. Soc. Jpn.* **2004**, *82*, 241–247.
23. Zhu, J. 80 Year oscillation of summer rainfall over North China and East Asian summer monsoon. *Geophys. Res. Lett.* **2002**, *29*, doi:10.1029/2001GL013997.
24. Minobe, S. A 50–70 year climatic oscillation over the north pacific and North America. *Geophys. Res. Lett.* **1997**, *24*, 683–686.
25. Sen Roy, S. A spatial analysis of extreme hourly precipitation patterns in India. *Int. J. Climatol.* **2009**, *29*, 345–355.
26. Zhang, K.; Pan, S.; Cao, L.; Wang, Y.; Zhao, Y.; Zhang, W. Spatial distribution and temporal trends in precipitation extremes over the hengduan mountains region, china, from 1961 to 2012. *Quat. Int.* **2014**, *349*, 346–356.
27. Chen, F.; Chen, H.; Yang, Y. Annual and seasonal changes in means and extreme events of precipitation and their connection to elevation over Yunnan province, China. *Quat. Int.* **2015**, in press.
28. Wu, C.H.; Huang, G.R.; Yu, H.J.; Chen, Z.Q.; Ma, J.G. Spatial and temporal distributions of trends in climate extremes of the feilaixia catchment in the upstream area of the Beijiang river basin, South China. *Int. J. Climatol.* **2014**, *34*, 3161–3178.
29. Wu, Y.J.; Wu, S.G.; Zhai, P.M. The impact of tropical cyclones on Hainan Island’s extreme and total precipitation. *Int. J. Climatol.* **2007**, *27*, 1059–1064.